ELECTRONIC SUPPORTING INFORMATION

Gold- and Silver-based Ionic liquids: effect of luminescence modulation depending on physical state.

Alexei Tokarev,[a] Joulia Larionova,[a] Yannick Guari,*[a] Christian Guérin,[a] José M. López-de-Luzuriaga,[b] Miguel Monge,*[b] Philippe Dieudonné,[c] Christophe Blanc[c]

[a] *Institut Charles Gerhardt Montpellier, UMR5253, Chimie Moléculaire et Organisation du Solide, Université Montpellier II, Place E. Bataillon, 34095, Montpellier cedex 5, France. Fax: 33 467143852; Tel: 33 467144224; E-mail: yannick.guari@univ-montp2.fr*

[b] *Departamento de Química, Universidad de La Rioja, Grupo de Síntesis Química de La Rioja, UA-CSIC, CCT-Madre de Dios 51, 26004-Logroño, Spain. Fax: 34 941299621; Tel: 34 941299644; E-mail: miguel.monge@unirioja.es*

[c] *Laboratoire des Colloïdes, Verres et Nanomatériaux, CNRS, UMR5587, Université de Montpellier II, 34095, Montpellier cedex 5, France.*

Synthesis.

[C_nMIM][BF_4] (with n = 12, 14 and 18) were synthesized according to previously published procedures.[2] [C_nMIM][$M(CN)_2$] (with n = 12, 14 and 18; M = Au, Ag) were by simple metathesis reactions involving precipitation from methanolic solutions from the corresponding [C_nMIM][BF_4] compounds.

In a typical synthesis, a methanolic solution (80 mL) of [C_{14}MIM][BF_4] (0.75 g, 2.05 mmol) was added to $KAu(CN)_2$ (0.59g, 2.05 mmol) and the mixture was stirred for one night at room temperature. The suspension was filtered off, the filtrate was concentrated (ca. 10 mL) and the product was precipitated by addition of Et_2O.

C_{18}MIM[$Au(CN)_2$] 1a. ^{13}C NMR (50 MHz, MeOD) δ (ppm): 144.480 (Au(*C*N)$_2$), 123.9-122.5 (N-*C*H-*C*H-N), 50.5 (-*C*H$_2$-N), 32.5 (N-*C*H$_3$), 31.3-20.6 (-*C*H$_2$-), 13.4 (-*C*H$_3$). ^{1}H NMR (200 MHz, MeOD) δ (ppm): 8.93 (1H, s, N-C*H*-N), 7.66-7.59 (2H, dd, N-C*H*-C*H*-N), 4.27-4.20 (2H, t, N-C*H*$_2$-), 3.96 (3H, s, N-C*H*$_3$), 1.96-1.32 (22H, m, -C*H*$_2$-), 0.96-0.90 (3H, t, -C*H*$_3$). IR (KBr disk, cm^{-1}): 2141, ν(CN). Mass spectrum: $[M – C_{18}mim]^-$ at m/z = 249.2, $[M – Au(CN)_2]^+$ at m/z = 335.5. Elemental analysis : Calc. For $C_{24}H_{43}N_4Au$: C, 49.31; H, 7.41; N, 9.58; Ag, 33.69. Found : C, 48.87; H, 7.22; N, 10.01; Ag, 33.87. [C_{18}MIM][$Au(CN)_2$] was obtained as a a white powder. Yield = 85 %.

C_{18}MIM[$Ag(CN)_2$] 1b. ^{13}C NMR (50 MHz, MeOD) δ (ppm): 144.4 (Ag(*C*N)$_2$), 123.9-122.6 (N-*C*H-*C*H-N), 49.8 (-*C*H$_2$-N), 35.4 (N-*C*H$_3$), 32.0-22.7 (-*C*H$_2$-), 13.4 (-*C*H$_3$); ^{1}H NMR (200 MHz, MeOD) δ (ppm): 8.93 (1H, s, N-C*H*-N), 7.67-7.60 (2H, dd, N-C*H*-C*H*-N), 4.28-4.21 [(2H, t, N-C*H*$_2$-), 3.96 (3H, s, N-C*H*$_3$), 1.97-1.32 (22H, m, -C*H*$_2$-), 0.97-0.90 3H, t, -C*H*$_3$). IR (KBr disk, cm^{-1}): 2130, ν(CN). Mass spectrum: $[M – C_{18}mim]^-$ at m/z = 159.9, $[M – Ag(CN)_2]^+$ at m/z = 335.5. Elemental analysis : Calc. For $C_{24}H_{43}N_4Ag$: C, 58.18; H, 8.75; N, 11.31; Ag, 21.77. Found : C, 58.47; H, 8.25; N, 11.07; Ag, 21.98. [C_{18}MIM][$Ag(CN)_2$] was obtained as a a white powder. Yield = 90 %.

C_{14}MIM[Au(CN)$_2$] 2a. ^{13}C NMR (50 MHz, MeOD) δ (ppm): 151.1 (Au(*C*N)$_2$), 123.9-122.6 (N-*C*H-*C*H-N), 49.9 (-*C*H$_2$-N), 35.4 (N-*C*H$_3$), 32.0-22.7 (-*C*H$_2$-), 13.4 (-*C*H$_3$). ^{1}H NMR (200 MHz, MeOD) δ (ppm): 8.94 (1H, s, N-C*H*-N), 7.64-7.58 (2H, dd, N-C*H*-C*H*-N), 4.22-4.20 (2H, t, N-C*H*$_2$-), 3.96-3.94 (3H, s, N-C*H*$_3$), 1.91-1.21 (22H, m, -C*H*$_2$-), 0.93-0.91 (3H, t, -C*H*$_3$). IR (KBr disk, cm^{-1}): 2143, ν(CN). Mass spectrum: [M – C_{12}mim]$^-$ at m/z = 249.2, [M – Au(CN)$_2$]$^+$ at m/z = 279.4. Elemental analysis : Calc. For $C_{20}H_{35}N_4Au$: C, 45.45; H, 6.68; N, 10.60; Au, 37.27. Found : C, 45.19; H, 6.73; N, 10.83; Au, 37.20. [C_{14}MIM][Au(CN)$_2$] was obtained as a white powder. Yield = 95 %.

C_{14}MIM[Ag(CN)$_2$] 2b. ^{13}C NMR (50 MHz, MeOD) δ (ppm): 144.4 (Ag(*C*N)$_2$), 123.9-122.6 (N-*C*H-*C*H-N), 49.8 (-*C*H$_2$-N), 35.4 (N-*C*H$_3$), 32.0-22.7 (-*C*H$_2$-), 13.4 (-*C*H$_3$). ^{1}H NMR (200 MHz, MeOD) δ (ppm): 8.94 (1H, s, N-C*H*-N), 7.64-7.60 (2H, dd, N-C*H*-C*H*-N), 4.27-4.20 (2H, t, N-C*H*$_2$-), 3.96 (3H, s, N-C*H*$_3$), 1.92-1.21 (22H, m, -C*H*$_2$-), 0.93-0.91 (3H, t, -C*H*$_3$). IR (KBr disk, cm^{-1}): 2139, ν(CN). Mass spectrum: [M – C_{14}mim]$^-$ at m/z = 159.9, [M – Ag(CN)$_2$]$^+$ at m/z = 279.4. Elemental analysis : Calc. For $C_{20}H_{35}N_4Ag$: C, 54.67; H, 8.03; N, 12.75; Ag, 24.55. Found : C, 54.27; H, 7.98; N, 12.90; Au, 24.83. [C_{14}MIM][Ag(CN)$_2$] was obtained as a a white powder. Yield = 90 %.

C_{12}MIM[Au(CN)$_2$] 3a. ^{13}C NMR (50 MHz, MeOD) δ (ppm): 144.6 (Au(*C*N)$_2$); 124.1-122.8 (N-*C*H-*C*H-N), 50.0 (-*C*H$_2$-N), 35.9 (N-*C*H$_3$), 32.2-22.9 (-*C*H$_2$-), 13.8 (-*C*H$_3$). ^{1}H NMR (200 MHz, MeOD) δ (ppm): 8.95 (1H, s, N-C*H*-N), 7.70-7.61 (2H, dd, N-C*H*-C*H*-N], 4.35-4.09 (2H, t, N-C*H*$_2$-), 3.99 (3H, s, N-C*H*$_3$), 1.99-1.32 (22H, m, -C*H*$_2$-], 0.93-0.88 (3H, t, Hz, -C*H*$_3$). IR (KBr disk, cm^{-1}): 2139, ν(CN). Mass spectrum: [M – C_{12}mim]$^-$ at m/z = 249.2, [M – Au(CN)$_2$]$^+$ at m/z = 251.4. Elemental analysis : Calc. For $C_{18}H_{31}N_4Au$: C, 43.20; H, 6.24; N, 11.20; Au, 39.36. Found : C, 43.02; H, 5.98; N, 10.89; Au, 38.75. [C_{12}MIM][Au(CN)$_2$] was obtained as a yellowish liquid. Yield = 82 %.

C_{12}MIM[Ag(CN)$_2$] 3b. ^{13}C NMR (50 MHz, MeOD) δ (ppm): 144.7 (Ag(*C*N)$_2$), 124.0-

122.8 (N-*C*H-*C*H-N), 50.0 (-*C*H$_2$-N), 35.9 (N-*C*H$_3$), 32.1-22.8 (-*C*H$_2$-), 13.8 (-*C*H$_3$). ^{1}H NMR (200 MHz, MeOD) δ (ppm): 8.97 (1H, s, N-C*H*-N), 7.68-7.60 (2H, dd, N-C*H*-C*H*-N), 4.34-4.08 (2H, t, N-C*H*$_2$-), 3.99 (3H, s, N-C*H*$_3$), 1.99-1.34 (22H, m, -C*H*$_2$-), 0.97-0.90 (3H, t, -C*H*$_3$). IR (KBr disk, cm^{-1}): 2132, ν(CN). Mass spectrum: [M – C$_{12}$mim]$^-$ at m/z = 159.9, [M – Ag(CN)$_2$]$^+$ at m/z = 251.4. Elemental analysis : Calc. For $C_{18}H_{31}N_4Ag$: C, 52.56; H, 7.60; N, 13.62; Ag, 26.22. Found : C, 52.23; H, 7.42; N, 13.47; Ag, 25.71. [C$_{12}$MIM][Ag(CN)$_2$] was obtained as a yellowish liquid. Yield = 89 %.

Physical Measurements

Elemental analyses were performed by the Service Central d'Analyse (CNRS, Vernaison, France). IR spectra were recorded on a Perkin Elmer 1600 spectrometer with a 4 cm^{-1} resolution. UV-Vis spectra were recorded in solid state on a Perkin Elmer Lambda 35 spectrometer. The melting points, clearing points, and glass-transition temperatures were determined by differential scanning calorimetry (NETZSCH PSC 204 F1 Phoenix equipped with dinitrogen cryostatic cooling, 5-15 mg samples, 2 °C min^{-1} heating and cooling rates), calibrated using an indium primary standard. The samples have been firstly heated to 70 °C and then cooled to -50 °C; then, the DSC measurements have been performed from -50 °C to 200 °C for the second and third cycles. The point at which the deviation from baseline starts is determined as the temperature transition. Optical characterization of the compounds and the detection of mesophases were performed with a polarizing microscope (Leitz 12 POL S) equipped with a 1024 pixel X 768 pixel Sony CCD camera and an Instec hot stage regulated at 0.1°C. Powder samples were deposited between slides and cover slips and inserted into the hot stage at room temperature. The temperature was then slowly increased (typically 1 °C/min), and the phase transition were detected from the texture changes observed between crossed polarizers. Once in the isotropic phase, the temperature was decreased, and the phase transitions under cooling were similarly detected. X-ray diffraction measurements on dried powders were carried out in 1.5-mm-diameter glass capillaries in a transmission configuration. A copper rotating anode X-ray source (functioning at 4 kW) with a multiplayer focusing Osmic monochromator giving high flux (10^8 photons/s) and punctual collimation was employed. An image plate 2D detector was used. X-ray diffractograms were obtained, giving the scattering intensity as a function of the wave vector q. A Mettler oven equipped with mylar windows was used for measurements at temperature between 22 and 100°C. Scattered intensity was corrected by exposition time, transmission, and intensity background coming from scattering by an empty capillary.

Excitation and emission spectra as well as lifetime measurements were recorded with a Jobin-Yvon Horiba Fluorolog 3-22 Tau-3 spectrofluorimeter . The samples at high temperatures were heated in quartz tubes on a mineral oil bath and measured on a quartz dewar.

Computational details

All calculations were performed using the Gaussian 03 suite of programs.[1]

Density Functional Theory DFT calculations were used for the full optimisation of the first triplet excited state of model system $[Emim]_2[Au(CN)_2]_2$ (Emim = 1-ethyl-3-methylimidazolium).

The 19-valence electron (VE) quasirelativistic (QR) pseudopotential (PP) of Andrae[2] was employed for gold together with two f-type polarization functions (exponents: 0.2, 1.19). The diffuse f-type function is required for describing the aurophilic attraction and the compact one for describing the covalent bonds.[3]

The atoms N and C were treated by Stuttgart pseudopotentials,[4] including only the valence electrons for each atom. For these atoms double-zeta basis sets of ref 4 were used, augmented by d-type polarization functions. For the H atom, a double-zeta, plus a p-type polarization function was used.[5]

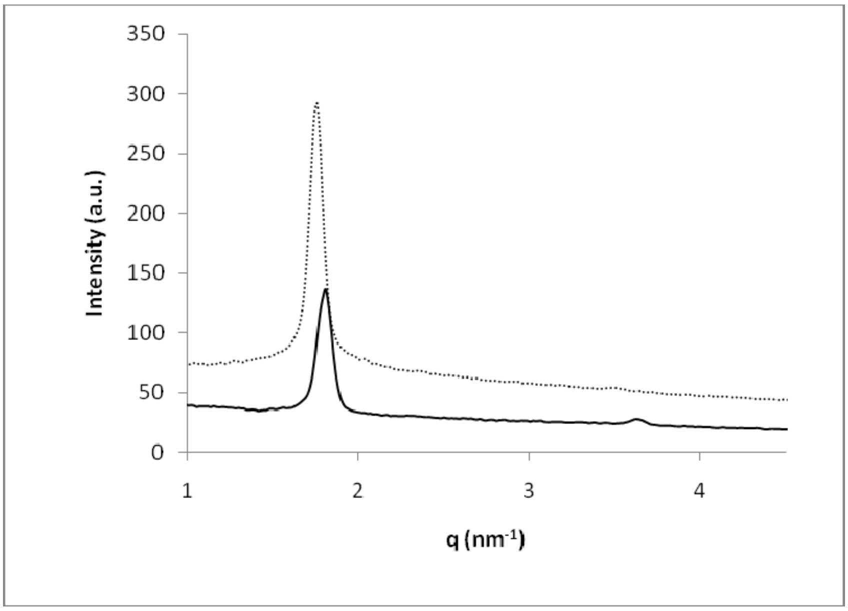

Figure 1S. X-ray diffractograms of sample (**1a**) in its liquid crystalline phase (80°C, dotted line) and its crystalline phase (22°C, solid line).

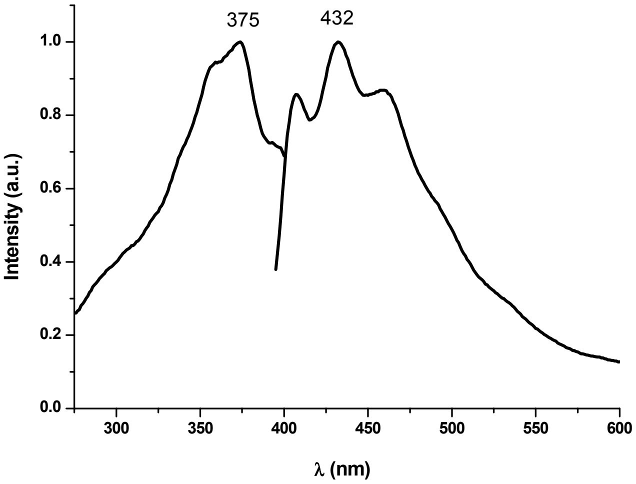

Figure 2S. Excitation and emission spectra of $[C_{18}MIM]BF_4$ salt in solid state at room temperature.

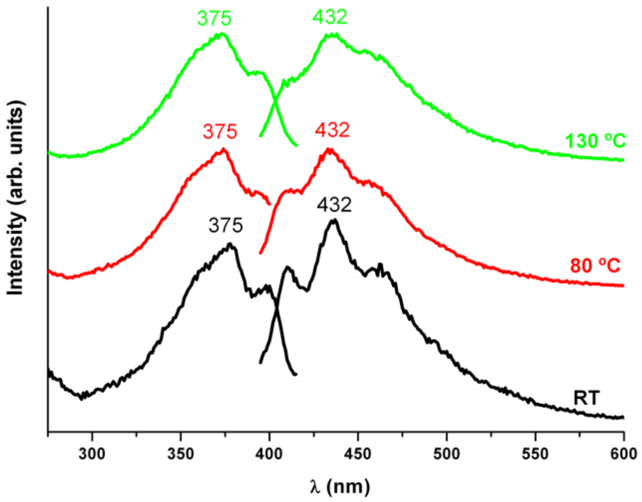

Figure 3S. Excitation and emission spectra of [C_{18}MIM][$Ag(CN)_2$] complex **1b** at different temperatures.

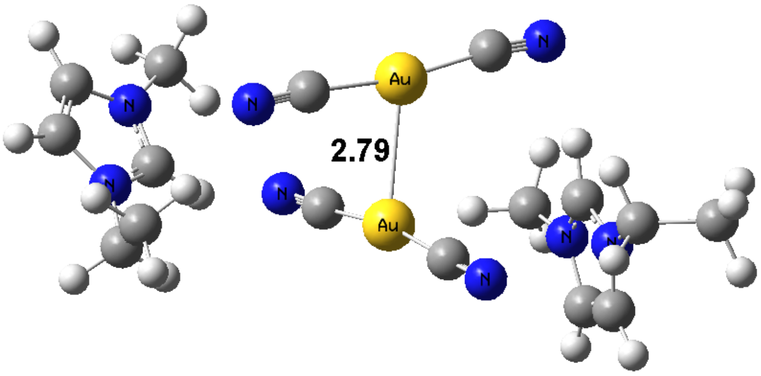

Figure 4S. Rearrangement of the [Emim]$_2$[$Au(CN)_2$]$_2$ model system upon photoexcitation and relaxation to the lowest triplet excited state T_1.

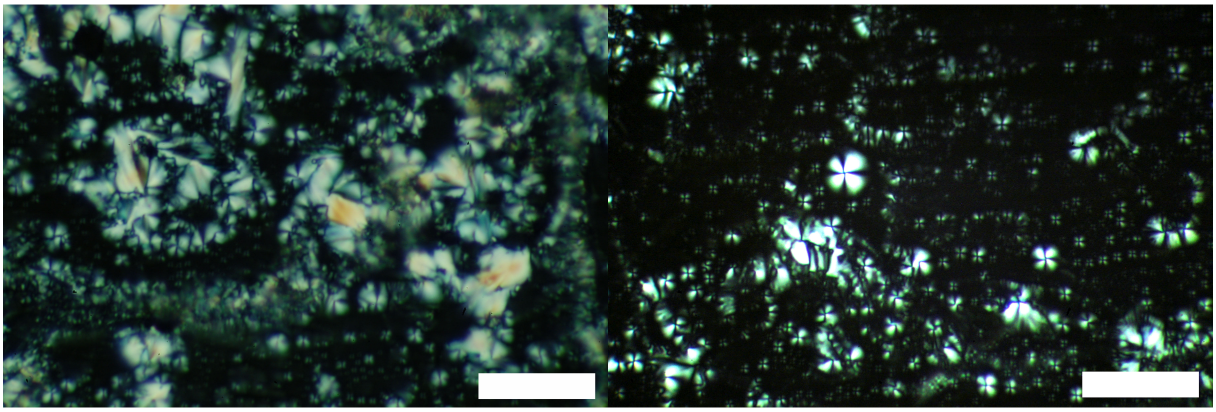

Figure 5S. Optical microscopy image (crossed polarizers) for **1b** taken in the crystaline phase at 22°C (left) and in the liquid crystalline phase at 90°C (right). Scale bars = 50 μm.

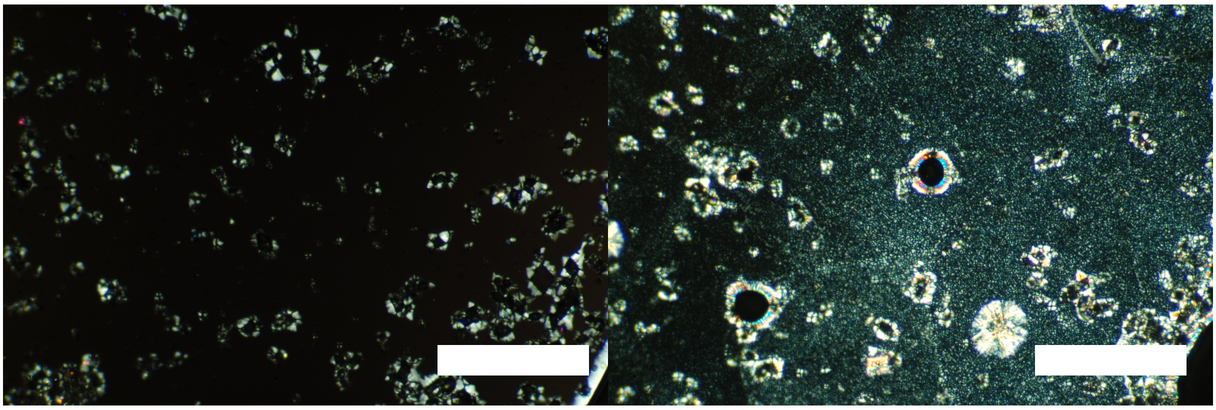

Figure 6S. Optical microscopy image (crossed polarizers) for **2a** taken at the Cr-LC transition when cooling at 21°C (left) and warming at 8°C (right). Scale bars = 50 μm.

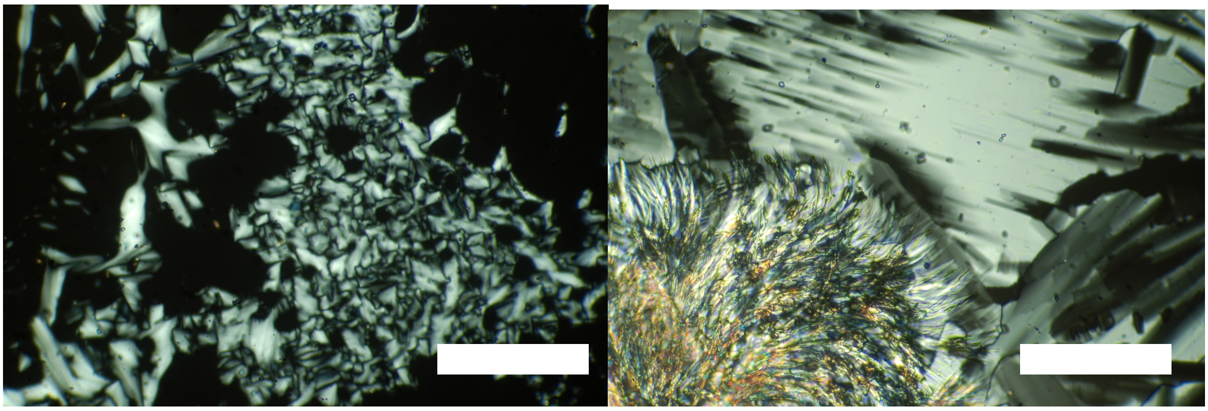

Figure 7S. Optical microscopy image (crossed polarizers) for **2b** taken at the Cr-LC transition when cooling at 32°C (left) and warming at 17°C (right). Scale bars = 50 μm.

IL	Treatment	Phase				
		Cr		SmA		I
3a	Cool		-23.8(9.0)		-21.1(2.7)	
	Heat		18.2(-43.3)		n.d.	
2a	Cool		11.1(33.6)		24.8(0.3)	
	Heat		23.0(-61.7)		n.d.	
1a	Cool		48.6(49.2)		89.9(n.d.)	
	Heat		47.2(-92.6)		106.3(-1.1)	
3b	Cool		-21.9(33.2)		-8.4(0.5)	
	Heat		-17.2(-34.7)		n.d.	
2b	Cool		13.4(39.3)		37.1(0.5)	
	Heat		23.6(-63.7)		37.8(-0.5)	
1b	Cool		49.4(51.5)		123.5(1.2)	
	Heat		48.4(-48.2)		129.2(-1.4)	

Table 1S. Thermal date from DSC of compounds **1a,b-3a,b**. Transition temperatures (°C) measured from the peak positions for first order transitions (*i.e.* melting and clearing points); enthalpy (J.g^{-1}) given in parentheses.

Although the SmA-Cr transition of all compounds displays always well-defined peaks, large thermal hysteresis are observed and the DSC traces suggest that the transition might have some glassy characteristics (see Fig.1).

References

[1] Gaussian 03, Revision C.02, Frisch, M. J.; Trucks, G. W.; Schlegel, H. B.; Scuseria, G. E.; Robb, M. A.; Cheeseman, J. R.; Montgomery, Jr., J. A.; Vreven, T.; Kudin, K. N.; Burant, J. C.; Millam, J. M.; Iyengar, S. S.; Tomasi, J.; Barone, V.; Mennucci, B.; Cossi, M.; Scalmani, G.; Rega, N.; Petersson, G. A.; Nakatsuji, H.; Hada, M.; Ehara, M.; Toyota, K.; Fukuda, R.; Hasegawa, J.; Ishida, M.; Nakajima, T.; Honda, Y.; Kitao, O.; Nakai, H.; Klene, M.; Li, X.; Knox, J. E.; Hratchian, H. P.; Cross, J. B.; Bakken, V.; Adamo, C.; Jaramillo, J.; Gomperts, R.; Stratmann, R. E.; Yazyev, O.; Austin, A. J.; Cammi, R.; Pomelli, C.; Ochterski, J. W.; Ayala, P. Y.; Morokuma, K.; Voth, G. A.; Salvador, P.; Dannenberg, J. J.; Zakrzewski, V. G.; Dapprich, S.; Daniels, A. D.; Strain, M. C.; Farkas, O.; Malick, D. K.; Rabuck, A. D.; Raghavachari, K.; Foresman, J. B.; Ortiz, J. V.; Cui, Q.; Baboul, A. G.; Clifford, S.; Cioslowski, J.; Stefanov, B. B.; Liu, G.; Liashenko, A.; Piskorz, P.; Komaromi, I.; Martin, R. L.; Fox, D. J.; Keith, T.; Al-Laham, M. A.; Peng, C. Y.; Nanayakkara, A.; Challacombe, M.; Gill, P. M. W.; Johnson, B.; Chen, W.; Wong, M. W.; Gonzalez, C.; and Pople, J. A.; Gaussian, Inc., Wallingford CT, 2004.

[2] Andrae, D.; Häusserman, U.; Dolg, M.; Stoll, H.; Preuss, H. *Theor. Chim. Acta* **1990**, *77*, 123.

[3] Pyykkö, P.; Runeberg, N.; Mendizabal, F. *Chem. Eur. J.* **1997**, *3*, 1451.

[4] Bergner, A.; Dolg, M.; Küchle, W.; Stoll, H.; Preuss, H. Mol. Phys. 1993, 80, 1431.

[5] Huzinaga, S. *Gaussian Basis Sets for Molecular Calculations*; Elsevier: Amsterdam, 1984; p16.